

# Improving the discovery potential of charged Higgs bosons at the Tevatron and Large Hadron Collider

Stefano Moretti

CERN Theory Division, CH-1211 Geneva 23, Switzerland and

Institute for Particle Physics Phenomenology, University of Durham, Durham DH1 3LE, UK

**Abstract.** We outline several improvements to the experimental analyses carried out at Tevatron (Run 2) or simulated in view of the Large Hadron Collider (LHC) that could increase the scope of CDF/D0 and ATLAS/CMS in detecting charged Higgs bosons.

**Keywords.** Charged Higgs bosons, hadron colliders, jets, leptons

**PACS Nos** 12.60.Fr, 13.85.-t, 13.87.-a, 14.60.-z

## 1. Introduction

The detection of charged Higgs bosons ( $H^\pm$ ) at Tevatron or the LHC would unequivocally imply the existence of physics beyond the Standard Model (SM), since spin-less charged scalar states do not belong to its particle spectrum. Singly charged Higgs bosons appear in any Two-Higgs Doublet Model (2HDM), including a Type-II in presence of minimal Supersymmetry (SUSY), namely, the Minimal Supersymmetric Standard Model (MSSM). In the latter scenario, these particles may be a unique probe of the ‘decoupling limit’, wherein the lightest scalar Higgs boson of the MSSM,  $h$ , is completely degenerate with the SM Higgs boson (i.e., same mass, couplings and physics properties in the interaction with ordinary matter), the other four Higgs states of the model,  $H$  (the heaviest scalar one),  $A$  (the pseudoscalar one) and the two charged ones, being much heavier, likewise for the new SUSY particles (squarks, sleptons and gauginos). A valuable introduction to charged Higgs boson physics at hadron colliders can be found in [1].

## 2. The top threshold region at Tevatron and the LHC

The Run 2 discovery potential of  $H^\pm$  bosons in a general Type-II 2HDM is visualised in Fig. 1 (from Sect. II.G of Ref. [2]). However, notice that the discovery reaches presented there ought to be considered as ‘conservative’. The reason being that they have been assessed by running Monte Carlo (MC) simulations of  $H^\pm$  production and decay channels that may severely underestimate the actual scope of charged Higgs boson searches. In fact, those estimates were made by assuming as main production mode of  $H^\pm$  scalars the

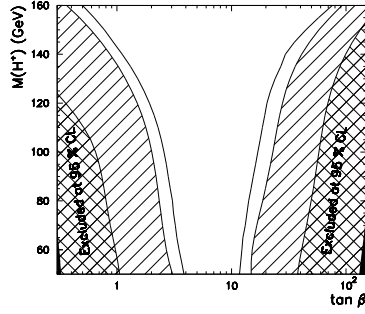


**Figure 1.** The D0/CDF combined 95% CL exclusion boundaries in the  $[M_{H^\pm}, \tan \beta]$  plane for several values of the integrated luminosity:  $0.1 \text{ fb}^{-1}$  (at  $\sqrt{s} = 1.8 \text{ TeV}$ , cross-hatched),  $2.0 \text{ fb}^{-1}$  (at  $\sqrt{s} = 2.0 \text{ TeV}$ , single-hatched) and  $10 \text{ fb}^{-1}$  (at  $\sqrt{s} = 2.0 \text{ TeV}$ , hollow).

decay of top (anti)quarks produced via QCD in the annihilation of gluon-gluon and quark-antiquark pairs (hence – by definition – the attainable Higgs mass is strictly confined to the region  $M_{H^\pm} < m_t = 175 \text{ GeV}$ ). This is not surprising, since standard MC programs, such as PYTHIA, HERWIG and ISAJET [], have historically accounted for this process through the usual procedure of factorising the production mode,  $gg, q\bar{q} \rightarrow t\bar{t}$ , times the decay one,  $\bar{t} \rightarrow \bar{b}H^-$ , in the so-called Narrow Width Approximation (NWA) []. This description fails to correctly account for the production phenomenology of charged Higgs bosons when their mass approaches or indeed exceeds that of the top-quark (i.e., falls in the ‘threshold region’,  $M_{H^\pm} \gtrsim m_t$ ). This is evident from the left plot in Fig. 2. As remarked in Ref. [], the use of the  $2 \rightarrow 3$  hard scattering process  $gg, q\bar{q} \rightarrow t\bar{b}H^-$  [], in place of the ‘factorisation’ procedure in NWA, is mandatory in the threshold region, as the former correctly keeps into account both the effect of the finite width of the top quark and the presence of other  $H^\pm$  production mechanisms, such Higgs-strahlung and  $b\bar{t} \rightarrow H^-$  fusion (and relative interferences). The differences seen between the two descriptions in the left plot of Fig. 2 are independent of  $\tan \beta$  and also survive in, e.g.,  $p_T$  and  $\eta$  spectra [].

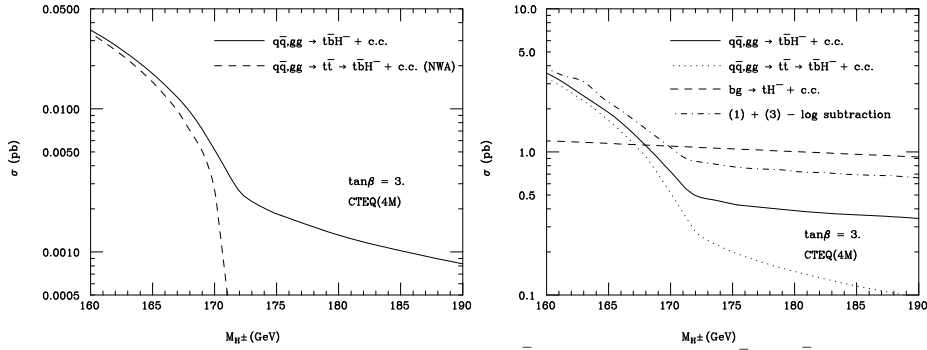


**Figure 2.** Cross section for  $gg, q\bar{q} \rightarrow t\bar{b}H^-$  and  $gg, q\bar{q} \rightarrow t\bar{t} \rightarrow t\bar{b}H^-$  in NWA, at the Tevatron with  $\sqrt{s} = 2 \text{ TeV}$  (left plot). Cross section for  $gg, q\bar{q} \rightarrow t\bar{b}H^-$ ,  $gg, q\bar{q} \rightarrow t\bar{t} \rightarrow t\bar{b}H^-$  with finite top quark width,  $bg \rightarrow tH^-$  and the combination of the first and the last, at the LHC with  $\sqrt{s} = 14 \text{ TeV}$  (right plot). Rates are function of  $M_{H^\pm}$  for a representative value of  $\tan \beta$ .

If one then looks at the most promising (and cleanest) charged Higgs boson decay channel, i.e.,  $H^\pm \rightarrow \tau^\pm \nu_\tau$  [], while reconstructing the accompanying top quark hadronically, the prospects of  $H^\pm$  detection improve significantly with increasing  $M_{H^\pm}$  values. By following the selection procedure outlined in Ref. [], one can establish at the Tevatron the presence of an  $H^\pm$  signal over the dominant (irreducible) background (that is,  $gg, q\bar{q} \rightarrow t\bar{b}W^- + \text{c.c.}$  events, yielding the same final state as the signal) up to masses of order  $m_t$ , hence in excess of 10 GeV or so with respect to the values in Fig. 1, for the same choice of  $\tan\beta$ : see Tab. 1 of []. The situation can be improved even further by taking advantage of  $\tau$ -polarisation effects, as explained in []. For example, by requiring that 80% of the  $\tau$ -jet (transverse) energy is carried away by the  $\pi^\pm$ 's in one-prong decays, one can reduce the background by a factor of 5, while costing to the signal only a more modest 50% reduction (for any  $M_{H^\pm}$  value between 160 GeV and  $m_t$ ).

The problematic just illustrated for the case of the Tevatron is very similar at the LHC, if anything more complicated. In fact, at the CERN hadron collider, the above  $2 \rightarrow 3$  reaction is dominated by the  $gg$ -initiated subprocesses, rather than by  $q\bar{q}$ -annihilation, as is the case at the Tevatron. This means that a potential problem of double counting arises in the simulation of  $t\bar{b}H^- + \text{c.c.}$  events at the LHC, if one considers that Higgs-strahlung can also be emulated through the  $2 \rightarrow 2$  process  $bg \rightarrow tH^- + \text{c.c.}$ , as was done in assessing the ATLAS discovery reaches in the  $H^+ \rightarrow t\bar{b}$  and  $H^+ \rightarrow \tau^+\nu_\tau$  channels []. The difference between the two approaches is well understood, and a prescription exists for combining the two, through the subtraction of a common logarithmic term: see Refs. []. The right plot in Fig. 2 summarises all the discussed issues in the context of the LHC. The mentioned  $2 \rightarrow 3$  description of the  $H^\pm$  production dynamics and the spin correlations in  $\tau$ -decays are now both available in version 6.4 of the HERWIG event generator (the latter also through an interface to TAUOLA []), so that detailed simulations of  $H^\pm$  signatures at both the Tevatron and CERN hadron colliders are now possible for the threshold region, including fragmentation/hadronisation and detector effects. Its adoption will ultimately allow to ‘naturally’ connect the discovery contours below and above the top threshold in the left plot of Fig. 3: the uncovered area at  $M_{H^\pm} \sim m_t$  (point 1.) is in fact an artifact of the simulations adopted in ATLAS (the same occurs in CMS: see right plot of Fig. 3).

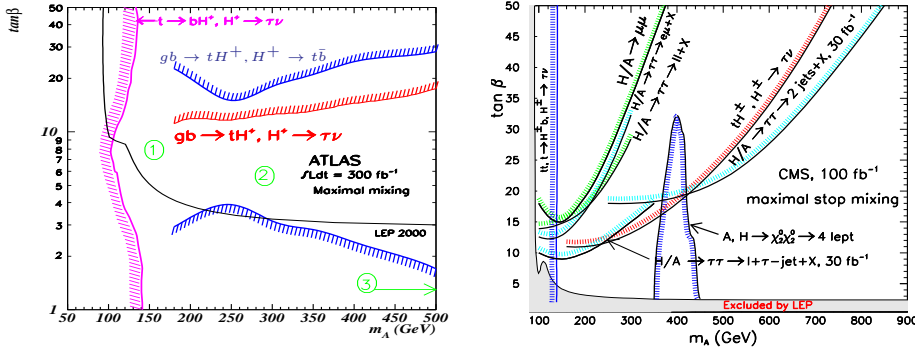


**Figure 3.** The ATLAS 5- $\sigma$  discovery contours of 2HDM charged Higgs bosons for  $300 \text{ fb}^{-1}$  of luminosity, only including the reach of SM decay modes (left plot). The CMS 5- $\sigma$  discovery contours of MSSM Higgs bosons for  $100 \text{ fb}^{-1}$  of luminosity, also including the reach of  $H, A \rightarrow \chi_2^0 \chi_2^0 \rightarrow 4l^\pm$  decays, assuming  $M_1 = 90 \text{ GeV}$ ,  $M_2 = 180 \text{ GeV}$ ,  $\mu = 500 \text{ GeV}$ ,  $M_{\tilde{g}} = 250 \text{ GeV}$ ,  $M_{\tilde{q}, \tilde{g}} = 1000 \text{ GeV}$  (right plot).

### 3. The intermediate $\tan\beta$ region at the LHC

The second uncovered region at the LHC in the  $[M_{H^\pm}, \tan\beta]$  plane (see point 2. in the left plot of Fig. 3) is precisely where the MSSM decoupling limit onsets. A possible means of accessing this area of the parameter space is to exploit SUSY decays of charged Higgs bosons [], similarly to what already done in CMS in the neutral sector (see right plot of Fig. 3) []. (For the impact of SUSY virtual effects see [1].) In particular, Ref. [1] showed that intermediate values of  $\tan\beta$  between 3 and 10 could be in part accessible via  $H^\pm \rightarrow \tilde{\chi}_1^\pm \tilde{\chi}_{\{2,3\}}^0$  modes, resulting in three lepton final states (where leptons mean electrons or muons), a hadronically reconstructed top quark (from  $gg \rightarrow \bar{b}tH^-$ ,  $gb \rightarrow tH^-$  and their c.c. production processes) plus substantial missing transverse momentum (from neutralino and chargino decays to the stable lightest neutralino,  $\tilde{\chi}_1^0$ , i.e., the lightest supersymmetric particle or LSP).

These signals have preliminarily been looked at in the context of the 2001 Les Houches workshop (second paper of [1]), in presence of a full (CMS) detector simulation (HERWIG 6.3 [2] was used to generate all hard processes). The results are rather promising, showing that all SM backgrounds can be completely removed, leaving only MSSM processes as irreducible backgrounds in the  $3\ell + p_T^{\text{miss}} + t$  channel ( $\ell = e, \mu$ ). Five MSSM points were considered, all in the intermediate  $\tan\beta$  region: see top of Tab. 3. (Here,  $M_1 = \frac{1}{2}M_2$  is assumed).

(Other MSSM parameters were:  $m_{\tilde{g}} = 700$  GeV,  $m_{\tilde{q}} = 1000$  GeV,  $m_{\tilde{b}_R} = 800$  GeV,  $m_{\tilde{t}_L} = 600$  GeV,  $m_{\tilde{t}_R} = 500$  GeV and  $A_t = 500$  GeV. Notice that rather large gluino and squark masses are chosen to preclude charged Higgs boson production from MSSM cascade decays [1], thus leaving the ‘direct’ production modes discussed so far as the only numerical relevant contributors at the LHC [1].)

Following the selection criteria outlined in Sect. G of the second paper in [1], one obtains the rates reported at the bottom of Tab. 3. Despite the limited  $XtH^-$  (and the c.c., after the subtraction of the common term) production rate precludes exploration for mass values larger than  $M_{H^\pm} \sim 300$  GeV, a signal could well be observed above the background, provided that: (i)  $\mu$  and  $M_2$  are not much above the current LEP restrictions from gaugino searches; (ii) sleptons are sufficiently light (to enhance the  $\tilde{\chi}_{\{2,3\}}^0 \rightarrow \tilde{\chi}_1^0 \ell^+ \ell^-$  decay rates). This is nonetheless a phenomenologically interesting parameter configuration as it will be promptly accessible at the LHC. More simulations are however still needed to assess the real potential of SUSY decays of charged Higgs bosons, without reducing the scope of the SM decay modes, whose BRs can be suppressed by the opening of the new channels.

### 4. The heavy mass region at the LHC

Point 3. in the left side of Fig. 3 refers to the possibility of increasing the  $H^\pm$  discovery potential of ATLAS and CMS in the  $H^+ \rightarrow \bar{t}b$  decay mode to charged Higgs masses much heavier than those considered so far. Following [1], the key is to exploit kinematical cuts on the  $b$ -quarks appearing in

$$gg, q\bar{q} \rightarrow b\bar{t}H^+ \rightarrow b\bar{t}t\bar{t} \rightarrow nbjj\ell^\pm p_T^{\text{miss}}, \quad (1)$$

where  $n = 3$  or  $4$ , with  $b$ -quarks being tagged. (Notice that if  $n = 3$ , the usual subtraction procedure has to be implemented, after accounting for the contribution from  $g\bar{b} \rightarrow \bar{t}H^+$

**Table 1.** Top: Simulated MSSM parameter points (all masses in GeV). The event number is the parton-level result for the production rates times the Branching Ratios (BRs) for  $H^\pm \rightarrow \chi_1^\pm \chi_{\{2,3\}}^0 \rightarrow 3\ell p_T^{\text{miss}}$  and  $t \rightarrow bj\bar{j}$  (where  $j$  represent a non- $b$ -jet). Bottom: Number of events after cuts. All rates are given at a luminosity of  $100 \text{ fb}^{-1}$ .

Point	$\tan \beta$	$m_{H^\pm}$	$\mu$	$M_2$	$m_{\tilde{t}_R}$	$m_{\tilde{t}_L}$	events
A	8	250	-115	200	120	170	1243
B	10	250	-115	200	120	170	1521
C	10	300	-115	200	120	170	1245
D	10	250	+130	210	125	175	1288
E	10	300	+130	210	125	175	1183

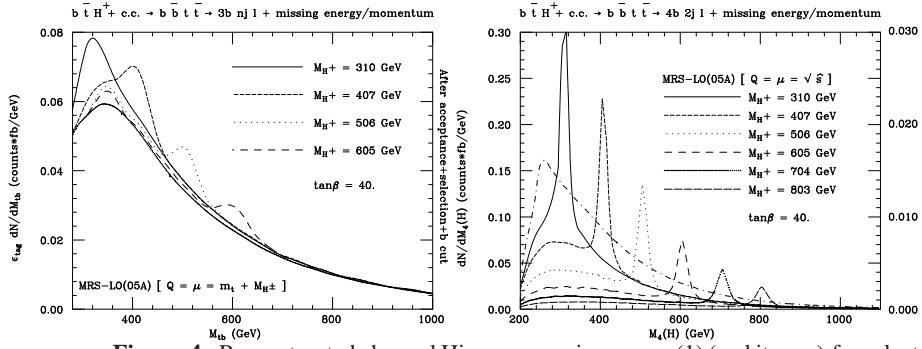
  

Process	$3\ell$ events	$Z^0$ -veto	3,4 jets	$m_{jjj} \sim m_t$	$M_{jj} \sim m_W^\dagger$	others
$t\bar{t}$	847	622	90	30	0	0
$t\bar{t}Z^0$	244	34	13	5	0	0
$t\bar{t}\gamma^*$	18	18	10	3	1	0
$t\bar{t}h$	66	52	33	9	3	1
$\tilde{\ell}\bar{\ell}$	5007	4430	475	112	2	0
$\tilde{\chi}\bar{\chi}$	8674	7047	1203	365	19	3
$\tilde{q}, \tilde{g}$	37955	29484	3507	487	100	0
$tH^+$ (point A)	251	241	80	23	6	5
$tH^+$ (point B)	321	298	118	42	13	9
$tH^+$ (point C)	279	258	100	36	11	7
$tH^+$ (point D)	339	323	121	48	13	9
$tH^+$ (point E)	291	278	114	40	10	5

<sup>†</sup>Includes  $b$ -tagging efficiency for the third jet

and c.c. too, whereas  $n = 4$  implies that the ‘spectator’  $b$ -quark in the  $2 \rightarrow 3$  mode has to enter the detector region.)

In both cases, an efficient  $b$ -tagging was assumed, in order to get rid of QCD backgrounds in light-quark- and gluon-jets. Whereas this is possible in the case of 3  $b$ -tags already for a single  $b$ -tagging efficiency of  $\epsilon_b \approx 0.4$  for any  $p_T(b) > 30 \text{ GeV}$ , in the case of 4  $b$ -tags the severe suppression induced onto the acceptance rates for process (1) by the requirement of detecting the spectator  $b$ -quark imposes  $\epsilon_b \approx 0.56$  for any  $p_T(b) > 20 \text{ GeV}$ . If these performances can be achieved by the ATLAS and CMS detectors, then charged Higgs resonances can be extracted from the backgrounds ( $t\bar{t}j$ ,  $t\bar{t}b$  and  $t\bar{t}b\bar{b}$ ) with large statistical significances up to 600–800 GeV or so, after simple kinematical cuts are applied on the  $b$ -quarks not generated in the two (anti)top-quark decays. Namely, by requiring either (i)  $p_T(b_3) > 30 \text{ GeV}$  in the case  $n = 3$  or (ii)  $M_{b_3b_4} > 120 \text{ GeV}$ ,  $\cos \theta_{b_3b_4} < 0.75$  and  $E_{b_3} > 120 \text{ GeV}$  in the case  $n = 4$  (where the subscripts identify the  $b$ -quarks in terms of their decreasing energy: i.e.,  $E_{b_3} > E_{b_4}$ ), one obtains the encouraging parton-level results displayed in Fig. 4 []. Here, the normalisation is to the total cross section of (1) times the number of possible ‘2  $b$  + 2 jet mass’ combinations: two in the left plot and and four in the right one. These findings still await confirmation through more realistic experimental analyses, but their potential in the high  $\tan \beta$  region is clearly evident.



**Figure 4.** Reconstructed charged Higgs masses in process (1) (and its c.c.) for selected values of  $M_{H^\pm}$  and  $\tan\beta = 40$ , after all cuts. Left plot is for the sum of signal and background, assuming 3  $b$ -tags. Right plot is for signal and background (dot-dashed) separately, assuming 4  $b$ -tags (here, the right scale is obtained after multiplying by  $\epsilon_b^4$ ).

## References

- [1] A. Djouadi, R. Kinnunen, E. Richter-Was, H.U. Martyn (conveners), hep-ph/0002258; D. Cavalli, A. Djouadi, K. Jakobs, A. Nikitenko, M. Spira, C.E.M. Wagner, W.-M. Yao (conveners), hep-ph/0203056.
- [2] M. Carena, J. Conway, H.E. Haber and J. Hobbs (conveners), hep-ph/hep-ph/0010338.
- [3] T. Sjöstrand, Comp. Phys. Comm. 82 (1994) 74; T. Sjöstrand, P. Edén, C. Friberg, L. Lönnblad, G. Miu, S. Mrenna and E. Norrbin, Comp. Phys. Commun. 135 (2001) 238.
- [4] G. Marchesini, B.R. Webber, G. Abbiendi, I.G. Knowles, M.H. Seymour and L. Stanco, Comput. Phys. Commun. 67 (1992) 465; G. Corcella, I.G. Knowles, G. Marchesini, S. Moretti, K. Odagiri, P. Richardson, M.H. Seymour and B.R. Webber, hep-ph/9912396; JHEP 0101 (2001) 010; hep-ph/0107071; hep-ph/0201201.
- [5] F.E. Paige, S.D. Protopopescu, H. Baer and X. Tata, hep-ph/9804321; hep-ph/9810440.
- [6] M. Guchait and S. Moretti, JHEP 0201 (2002) 001.
- [7] J.F. Gunion, Phys. Lett. B322 (1994) 125; J.L. Diaz-Cruz and O.A. Sampayo, Phys. Rev. D50 (1994) 6820.
- [8] S. Moretti and W.J. Stirling, Phys. Lett. B347 (1995) 291; Erratum, ibidem B366 (1996) 451; A. Djouadi, J. Kalinowski and P.M. Zerwas, Z. Phys. C70 (1996) 435; E. Ma, D.P. Roy and J. Wudka, Phys. Rev. Lett. 80 (1998) 1162.
- [9] S. Raychaudhuri and D.P. Roy, Phys. Rev. D52 (1995) 1556.
- [10] K. A. Assamagan, Y. Coadou and A. Deandrea, hep-ph/0203121.
- [11] F. Borzumati, J.-L. Kneur and N. Polonsky, Phys. Rev. D60 (1999) 115011.
- [12] S. Moretti and D.P. Roy, Phys. Lett. B470 (1999) 209.
- [13] A. Belyaev, D. Garcia, J. Guasch and J. Solá, Phys. Rev. D65 (2002) 031701; hep-ph/0203031.
- [14] S. Jadach, Z. Was, R. Decker and J.H. Kuhn, Comput. Phys. Commun. 76 (1993) 361; M. Jezabek, Z. Was, S. Jadach and J.H. Kuhn, Comput. Phys. Commun. 70 (1992) 69; S. Jadach, J.H. Kuhn and Z. Was, Comput. Phys. Commun. 64 (1990) 275.
- [15] M. Bisset, M. Guchait and S. Moretti, Eur. Phys. J. C19 (2001) 143.
- [16] H. Baer, M. Bisset, X. Tata and J. Woodside, Phys. Rev. D46 (1992) 303.
- [17] S. Moretti, K. Odagiri, P. Richardson, M.H. Seymour and B.R. Webber, hep-ph/0204123.
- [18] A. Datta, A. Djouadi, M. Guchait and Y. Mambrini, Phys. Rev. D65 (2002) 015007.
- [19] S. Moretti, hep-ph/0102116.
- [20] D.J. Miller, S. Moretti, D.P. Roy and W.J. Stirling, Phys. Rev. D61 (2000) 055011.